

Structural Transitions of the $\text{CaF}_2/\text{Si}(111)$ Interface

C. A. Lucas, G. C. L. Wong,^(a) and D. Loretto

Center for Advanced Materials, Materials Sciences Division, Lawrence Berkeley Laboratory, University of California, Berkeley, California 94720

(Received 9 November 1992)

We have used x-ray reflectivity and transmission electron microscopy to study the $\text{CaF}_2/\text{Si}(111)$ interface. The results are consistent with a reconstructed two-layer CaF interface which can be transformed to a different structure simply by increasing the thickness of the CaF_2 overlayer. We are able to reconcile previous measurements of the interface structure and gain insight into the rich variety of phenomena that may be observed at heteroepitaxial interfaces.

PACS numbers: 61.16.Bg, 61.10.-i, 68.35.Rh, 68.55.Jk

$\text{CaF}_2/\text{Si}(111)$ is a prototypical system for studying atomic and electronic structure at the ionic/covalent interface. As a consequence there has been a wide range of experiments aimed at determining the interface structure and a number of models have been proposed [1,2]. Despite this attention no consistent picture has emerged. Conflicting results have been attributed to differences in sample preparation and the varying sensitivity of experimental techniques [3-5]. The problem relates to more general issues concerning the differences between surface and interface structure. In particular, it is questionable whether the structure observed at monolayer coverages, which is accessible to many standard surface probes, is representative of the true interface between two materials [6]. The latter can only be studied with techniques that employ highly penetrating beams, such as x-ray diffraction and transmission electron microscopy (TEM). It is the structure of the buried interface that influences the electronic properties.

In this Letter we present x-ray diffraction and TEM measurements of the $\text{CaF}_2/\text{Si}(111)$ interface. The results are consistent with a reconstructed two-layer CaF interface between the top Si double layer and the "bulklike" CaF_2 film. The interface structure is a metastable phase formed in the early stages of heteroepitaxy. By increasing the thickness of the CaF_2 film it is possible to drive a transition to a single layer CaF interface. Our results are consistent with previous experiments and reconcile many of the differences in proposed interface models. The results indicate that the rich variety of phenomena observed at surfaces, e.g., reconstructions and phase transitions, may also be observed at buried interfaces.

CaF_2 was grown by molecular beam epitaxy (MBE) on well-oriented (miscut $< 0.5^\circ$) $\text{Si}(111)$ substrates in an ISA/Riber CBE 32P ultrahigh vacuum (UHV) system. The Shiraki etched Si substrates [7] were outgassed thoroughly and then heated to 880°C to remove the protective oxide. Cooling to the growth temperature (720°C) routinely resulted in a sharp (7×7) reflection high-energy electron diffraction (RHEED) pattern. CaF_2 was deposited by evaporation from an effusion cell at 1150°C . During deposition the pressure was typically $\sim 1 \times 10^{-10}$ torr at a growth rate of ~ 1 CaF_2 triple layer (TL) per

30 s. At 720°C CaF_2 films with a thickness of ~ 7 TL's ($\sim 22 \text{ \AA}$) were grown. This is below the critical thickness for strained layer growth (~ 12 TL's). The sample was then cooled to room temperature where, due to the smaller lattice mismatch, it is possible to grow more CaF_2 in a layer-by-layer mode without introducing strain relieving dislocations. Using this "template" method pseudomorphic growth has been achieved up to a thickness of ~ 60 TL's. Samples were capped with 50 \AA of amorphous Si before removal from the vacuum.

X-ray reflectivity is a powerful technique for determining surface structure and has been employed with considerable success in studies of reconstructed metal surfaces [8,9]. The technique is analogous to LEED or RHEED measurements of the (00) specular rod, but the weak interaction of x rays with matter enables use of the kinematical approximation to scattering theory, in the form of a one-dimensional Fourier summation over the layers of the crystal [10]. Figure 1 shows the reflectivity

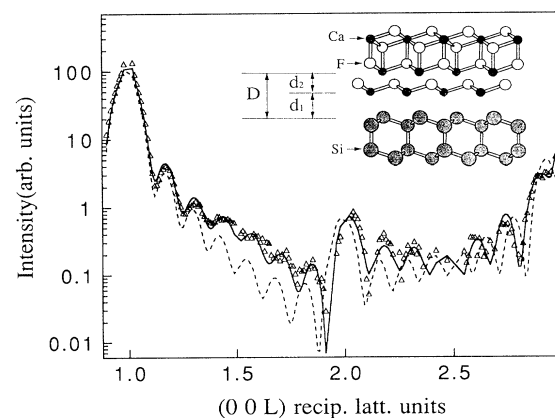


FIG. 1. Measured x-ray reflectivity of a 7 triple layer (TL) $\text{CaF}_2/\text{Si}(111)$ film. The data points are background subtracted integrated intensities corrected for the Lorentz factor and the variation in illuminated sample area. The dashed line is a calculation with a simple interface model (interface spacing $D = 4.55 \text{ \AA}$). The solid line is a fit to the data with a two-layer interface according to the parameters in Table I. Inset: A schematic illustration of the proposed interface structure.

profile for a 7 TL thick CaF_2 film (the film thickness is determined by the oscillation period). The measurement was performed on beam line 7-2 at the Stanford Synchrotron Radiation Laboratory using a 4-circle Huber diffractometer and a focused 1 mm (vertical) \times 2 mm (horizontal) incident x-ray beam ($\lambda = 1.2398 \text{ \AA}$). The sample was mounted at the center of the diffractometer axes, with its surface normal in the vertical scattering plane. Scattered x rays were detected by a scintillation counter after passing through 6 mm (vertical) \times 10 mm (horizontal) slits at a distance of ~ 1 m from the sample. Each point corresponds to a background subtracted integrated intensity obtained from θ scans at the appropriate 2θ scattering angle along the specular rod and the points are shown as a function of the hexagonal reciprocal lattice vector, L (where $[00L]_{\text{hex}} = [111]_{\text{cubic}}$). No data were collected for $L < 0.9$ reciprocal lattice units, due to scattering from the amorphous Si cap which affects the low angle reflectivity data, or over the range $L = 0.98 - 1.02$.

In a previous paper we presented similar x-ray scattering measurements from $\text{CaF}_2/\text{Si}(111)$, over a reduced range of L (0.8–1.2) around the Si(111) Bragg reflection [11]. Over this L range good fits to the data were obtained with a lattice separation $D = 4.55 \text{ \AA}$. The measurement is not sensitive to the detailed interface structure [12] and the large d value implies that there is a layer in between the two lattices. The dashed line in Fig. 1 corresponds to a simulation with the 4.55 \AA interface spacing. The calculated intensity is given by the modulus squared of the structure factor $F(q)$, where

$$F(q) = f_{\text{Si}}(q) \sum_{j=-\infty}^0 \exp(iqz_j) + \exp(iqD) \times \{f_{\text{Ca}}(q) + 2f_{\text{F}} \cos(qc/4)\} \sum_{k=0}^N \exp(iqz_k).$$

$f_{\text{Si}}(q)$, $f_{\text{Ca}}(q)$, and $f_{\text{F}}(q)$ are atomic form factors which include the Debye-Waller factor [13], z_j are the atomic height coordinates, c is the lattice spacing of the CaF_2 film with a thickness of N triple layers, and D is the inter-

face separation. Although the model fits the data around the (111) Bragg reflection it is clearly not a good fit to the data over the larger q range. Between Bragg reflections the scattering from atoms in bulk positions interferes destructively and is roughly equal in intensity to the scattering from an isolated monolayer [14]. The measurement is thus sensitive to the details of the interface structure projected onto the surface normal direction. An isolated monolayer at the interface is simple to include in the scattering model with an additional multiplying factor ρ_j representing a possible partial layer occupation (i.e., ρ_j varies between 0 and 1). Strain in the interface region can be accounted for by allowing the bulk layers to move away from their ideal positions. There are a number of constraints which must be imposed on the modeling procedure: We look for a model which has physically reasonable bond lengths and is consistent with previous results. It has been shown that upon initial adsorption the CaF_2 molecule dissociates to give a submonolayer coverage of CaF [1,4,5]. We can reproduce our data by including a CaF layer at the interface but this results in a Si-Ca separation of $\sim 1.6 \text{ \AA}$, which is not compatible with the Ca-Si bond length (3.0–3.2 \AA) [15]. The best fit to the data with a two-layer interface (the next simplest model) is shown by the solid line in Fig. 1. The structural parameters are given in Table I. The Ca-Si interface separation ($d_1 = 2.7 \text{ \AA}$) agrees with the ion-scattering results of Tromp and Reuter [1]. A partial occupation (46%) of CaF at threefold hollow sites (T4/H3) is more than sufficient to saturate the Si dangling bonds. However, the vertical separation between the CaF at the interface and the next layer is too small to accommodate CaF_2 in the second layer. If we assume a second layer of CaF we obtain a good fit to the data with a partial occupation of 65% in the second layer and bulk CaF_2 stacking above this. The interlayer spacing implies that the CaF bond lengths are slightly larger than in bulk CaF_2 . The different bond length for Ca-F, when Ca is in the +1 valence state rather than the +2 state found in CaF_2 , is not unexpected. The angular rigidity of covalent bonding is not a feature of ionic materials where the bonding can

TABLE I. Parameters to the fit to the x-ray reflectivity data shown by the solid line in Fig. 1.

Layer	Occupation ρ_j	Displacement from ideal position (\AA)	Comments
Top Si double layer	1	$\Delta_{\text{Si}} = 0 \pm 0.1$	Displacement towards the free surface
CaF (layer 1)	0.46 ± 0.2	$d_1 = 2.7 \pm 0.1$	Center of Si double layer to Ca atom
CaF (layer 2)	0.65 ± 0.2	$\Delta_{\text{F}} = 0$ $d_2 = 2.2 \pm 0.1$	i.e., F atom at $d_1 + c/4 + \Delta_{\text{F}}$ Ca (layer 2)-Ca (layer 1)
CaF_2 (first layer)	1	$\Delta_{\text{CaF}_2} = -0.4 \pm 0.2$ $\Delta_{\text{CaF}_2} = -0.3 \pm 0.1$	i.e., F atom at $d_2 + c/4 + \Delta_{\text{F}}$ Ca-Ca (layer 2) = $c + \Delta_{\text{CaF}_2}$
Number of CaF_2 layers, $N = 7$ $c = 3.170 \pm 0.008 \text{ \AA}$ $a_{\text{hex}}(\text{Si}) = 3.13559 \text{ \AA}$			

be thought of as a low-energy packing of charged spheres.

Figure 2(a) shows a two-beam, bright-field transmission electron micrograph taken from a 23 TL thick CaF_2 film where 7 TL's were grown at $\sim 720^\circ\text{C}$ followed by ~ 16 TL's at room temperature. Most of the line defects show contrast consistent with a displacement along $[11\bar{2}]$ [some additional threading line defects, with a different displacement, are visible in Fig. 2(a)]. Such line defects are anticipated at $\frac{1}{3}[111]$ steps on the Si substrate as a consequence of differences between the symmetry operators of the Si and the B-type CaF_2 . The presence of so few defects indicates that the in-plane lattice parameter of the CaF_2 film is matched to that of the Si substrate. This agrees with the x-ray diffraction experiments which show an increase in the (111) CaF_2 lattice parameter. Furthermore, the presence of so few defects suggests an atomically smooth interface. This is also in agreement with the x-ray data, which can be modeled without atomic scale roughness.

Figure 2(b) shows part of a $[111]$ transmission electron diffraction (TED) pattern taken at 200 keV from a 18 TL thick CaF_2 layer. The brightest peaks are reciprocal lattice points which have a nonzero structure factor for bulk Si and CaF_2 . Weaker peaks at $\frac{1}{3}\langle 224 \rangle$ are disallowed for the bulk but are allowed at a (111) interface/surface. The weakest features in $\frac{1}{3}\langle 220 \rangle$ positions are consistent with a $(\sqrt{3}\times\sqrt{3})R30^\circ$ unit cell ($\sqrt{3}$ for short), indexed using the Si surface unit cell. It is easy to construct this symmetry in a partially occupied layer and the result therefore supports the x-ray scattering model. During growth the $\sqrt{3}$ symmetry is not observed. As the coverage increases the RHEED pattern changes in the sequence $(7\times 7)\rightarrow(3\times 1)\rightarrow(4\times 1)\rightarrow(1\times 1)$. This implies that the interface is ordered differently when it is first grown from when it is buried under the CaF_2 film.

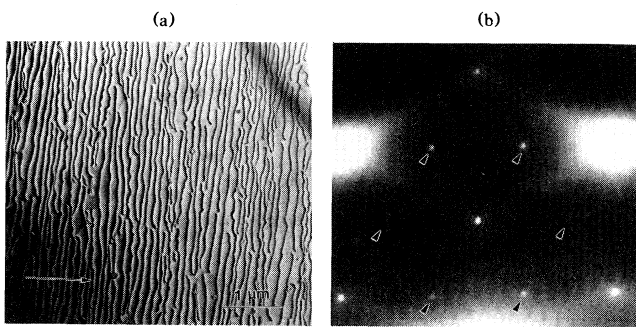


FIG. 2. (a) A bright-field TEM image taken from a 23 TL thick CaF_2 grown using the "template" method. The $[220]$ diffraction vector is marked. (b) Part of a $[111]$ transmission electron diffraction (TED) pattern taken at 200 keV from an 18 TL thick CaF_2 layer. The three brightest peaks are "bulk" Si and CaF_2 reciprocal lattice points in $\langle 220 \rangle$ positions. Peaks at $\frac{1}{3}\langle 224 \rangle$ arise from the (111) interface/surface. The features marked with arrows lie close to $\frac{1}{3}\langle 220 \rangle$ positions and can be attributed to a reconstructed layer at the $\text{CaF}_2/\text{Si}(111)$ interface.

Figure 2(b) shows that the reflections lying along radial directions through the Si $\langle 220 \rangle$ reflections are much weaker than those between Si $\langle 220 \rangle$ peaks. This canceling in the structure factor could result from the superposition of two supercells from the two layer CaF interface. A more detailed examination of the reflection positions in Fig. 2(b) reveals that they are systematically displaced from the $\sqrt{3}$ positions. Preliminary grazing incidence x-ray diffraction measurements confirm the TED results [16]. One surface reflection was measured, displaced from the $\sqrt{3}$ position and accompanied by regularly spaced satellite peaks. This scattering could be explained by the existence of stress domains, driven by an anisotropic stress on a high symmetry surface [17], leading to a weakly incommensurate interface phase [18].

The $\text{CaF}_2/\text{Si}(111)$ interface described above is consistent with previous ion scattering [1] and x-ray standing wave measurements [3] of submonolayer coverages, which indicated that CaF is adsorbed on threefold hollow sites (T4/H3). This corresponds to the CaF -Si composite surface, the first layer of the two-layer interface. Our study of the initial stages of growth showed that the CaF -Si composite surface is progressively covered by coherently strained islands, ~ 3 TL's thick, which eventually form a uniform epitaxial layer of CaF_2 [19]. The transition from the reconstruction observed by RHEED to the $\sqrt{3}$ structure must occur during the formation of the overlayer. It is possible that the existence of the two-layer interface is a consequence of the kinetic constraints against rehybridization, after the Si bonds have been saturated (which requires only $\frac{1}{3}$ of a monolayer of CaF). This suggests that the interface may not be at a global energy minimum.

A structural transition from the metastable two-layer interface to a single-layer one is observed. Figure 3 shows x-ray diffraction measurements of three samples, over the range $L=0.9-1.1$. The measurements were taken using a 4-circle diffractometer operating in a triple crystal mode based on a Rigaku 12 kW rotating anode x-ray source ($\lambda=1.54 \text{ \AA}$). The samples were prepared using the template growth method described above. From the oscillation period the film thicknesses are calculated as 20 and 33 TL for (a) and (b), respectively. Plan view TEM measurements produced identical results to Fig. 2(a) indicating that neither film has relaxed. Apart from the oscillation period there is a striking difference between the two data sets, namely, the asymmetry around the Bragg reflection in Fig. 3(b). This asymmetry is also observed in Fig. 3(c), measured from the same 23 TL sample as is shown in Fig. 2(a), which was heated to 400°C after CaF_2 growth. In the simple scattering model, where contributions from monolayers at the interface are ignored, the asymmetry is sensitively controlled by the interface separation d [11,12]. Solid lines in Fig. 3 are fits to the data using this model. For Figs. 3(b) and 3(c) $D=2.9\pm 0.1 \text{ \AA}$ [compared with $D=4.55 \text{ \AA}$ for Fig. 3(a)]. This value is consistent with a single interface and

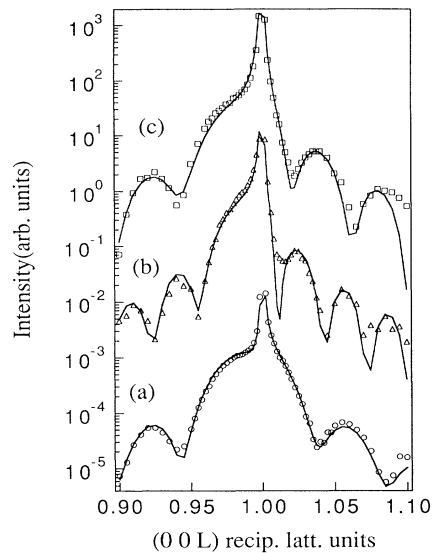


FIG. 3. X-ray reflectivity around the Si(111) Bragg reflection for CaF_2 films grown using a template method to a thickness of (a) 20, (b) 33, and (c) 23 TL. The data in (c) were taken after the sample was heated to 400°C . The solid lines are fits to the data with a single CaF layer at the interface and an interface spacing (i.e., from the middle of the top Si double layer to the Ca atom) of (a) $D=4.55 \text{ \AA}$ and (b),(c) $D=2.9 \pm 0.1 \text{ \AA}$. Each data set is displaced for clarity.

a full CaF layer at a bulk CaF_2 lattice position.

The structural transition is driven by the coherent strain applied at the interface by the CaF_2 epilayer. Unrelaxed films of the same thickness (19 TL's) can be prepared with the two different interface structures. For example, two films grown by the template method, with homoepitaxial growth at room temperature in one case, and at 430°C in the other have different interfaces. The film grown at room temperature shows the two-layer interface. The additional strain in the 430°C film drives the interface transition. Furthermore, we are unable to observe the transition in unrelaxed samples grown isothermally at 720°C , even though the lattice mismatch is large. At 720°C a film will relax at 12 TL's before the transition is induced. However, a thick enough relaxed 720°C film will eventually build up enough residual strain to drive the transition [20]. The transition also occurs if the sample is heated after growth [Fig. 3(c)] due to the increase in lattice mismatch. This may explain the structural changes, caused by rapid thermal anneal, that were observed by Batstone, Phillips, and Hunke [2] and attributed to a loss of interfacial fluorine.

To summarize, we have reconciled the discrepancies between previous models of the $\text{CaF}_2/\text{Si}(111)$ interface. We propose a two-layer interface which undergoes transition to a different energy structure. The results call into

question traditional assumptions regarding the similarities between surface and interface structures and indicate that a variety of interesting phenomena may be observed at heteroepitaxial interfaces.

We are grateful to Phil Cullen for technical assistance and to Tai Nguyen for help at SSRL. D.L. acknowledges the National Center for Electron Microscopy for use of its microscopes. We also thank the staff and user administration at SSRL for their hospitality and, in particular, Sean Brennan for his support on beam line 7-2. SSRL is operated by the Department of Energy, Division of Chemical Sciences. This work was supported by the Director, Office of Basic Energy Sciences, Materials Sciences Division of the U.S. Department of Energy under Contract No. AC03-76SF00098.

(a)Also at Department of Physics, University of California, Berkeley, CA 94720.

- [1] R. M. Tromp and M. C. Reuter, *Phys. Rev. Lett.* **61**, 1756 (1988).
- [2] J. L. Batstone, J. M. Phillips, and E. C. Hunke, *Phys. Rev. Lett.* **60**, 1394 (1988).
- [3] J. Zegenhagen and J. R. Patel, *Phys. Rev. B* **41**, 5315 (1990).
- [4] Ph. Avouris and R. Wolkow, *Appl. Phys. Lett.* **55**, 1074 (1989).
- [5] M. A. Olmstead *et al.*, *Phys. Rev. B* **35**, 7526 (1987).
- [6] H. Hong *et al.*, *Phys. Rev. Lett.* **68**, 507 (1992).
- [7] A. Ishizaka and Y. Shiraki, *J. Electrochem. Soc.* **133**, 666 (1986).
- [8] D. Gibbs, B. M. Ocko, D. M. Zehner, and S. G. J. Mochrie, *Phys. Rev. B* **38**, 7303 (1988).
- [9] B. M. Ocko, D. Gibbs, K. G. Huang, D. M. Zehner, and S. G. J. Mochrie, *Phys. Rev. B* **44**, 6429 (1991).
- [10] I. K. Robinson and E. Vlieg, *Surf. Sci.* **261**, 123 (1992).
- [11] C. A. Lucas and D. Loretto, *Appl. Phys. Lett.* **60**, 2073 (1992).
- [12] I. K. Robinson, R. T. Tung, and R. Feidenhans'l, *Phys. Rev. B* **38**, 3632 (1988).
- [13] The atomic form factors are obtained from polynomial fits to the values given in *The International Tables for X-Ray Crystallography* (Kynoch Press, Birmingham, England, 1968), Vol. 3'.
- [14] I. K. Robinson and D. J. Tweet, *Rep. Prog. Phys.* **55**, 599 (1992).
- [15] C. G. Van de Walle, *Phys. Rev. B* **43**, 11913 (1991).
- [16] Experiments were performed on beamline 7-2 at SSRL with the crystallographic alignment determined by several in-plane Si Bragg reflections.
- [17] O. L. Alerhand *et al.*, *Phys. Rev. Lett.* **61**, 1973 (1988).
- [18] P. W. Stephens *et al.*, *Phys. Rev. B* **29**, 3512 (1984).
- [19] G. C. L. Wong, D. Loretto, and C. A. Lucas (unpublished).
- [20] For a discussion of strain effects see, for example, the two volumes of *Strained-Layer Superlattices*, edited by T. M. Pearsall (Academic, San Diego, CA, 1991).

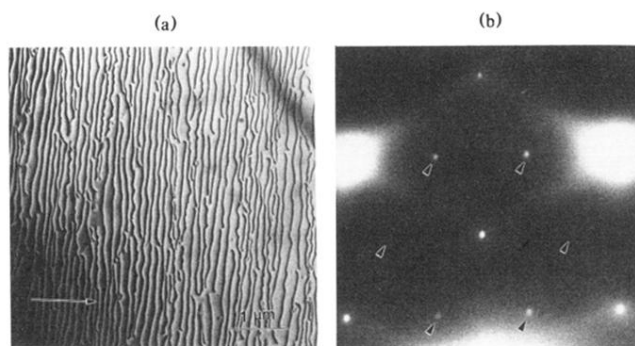


FIG. 2. (a) A bright-field TEM image taken from a 23 TL thick CaF_2 grown using the “template” method. The $[220]$ diffraction vector is marked. (b) Part of a $[111]$ transmission electron diffraction (TED) pattern taken at 200 keV from an 18 TL thick CaF_2 layer. The three brightest peaks are “bulk” Si and CaF_2 reciprocal lattice points in $\langle 220 \rangle$ positions. Peaks at $\frac{1}{3}\langle 224 \rangle$ arise from the (111) interface/surface. The features marked with arrows lie close to $\frac{1}{3}\langle 220 \rangle$ positions and can be attributed to a reconstructed layer at the $\text{CaF}_2/\text{Si}(111)$ interface.